Biochimica et Biophysica Acta 1804 (2010) 184–192

Contents lists available at ScienceDirect

Biochimica et Biophysica Acta

journal homepage: www.elsevier.com/locate/bbapap

Structure and characterization of amidase from *Rhodococcus* sp. N-771: Insight into the molecular mechanism of substrate recognition

Akashi Ohtaki [a,1], Kensuke Murata [a,1], Yuichi Sato [a], Keiichi Noguchi [a], Hideyuki Miyatake [b], Naoshi Dohmae [b], Kazuhiro Yamada [a], Masafumi Yohda [a,*], Masfumi Odaka [a]

[a] *Department of Biotechnology and Life Science, Tokyo University of Agriculture and Technology, 2-24-16 Naka-cho, Koganei, Tokyo 184-8588, Japan*
[b] *Biomolecular Characterization Team, Advanced Development and Supporting Center, RIKEN, 2-1 Hirosawa, Wako, Saitama 351-0198, Japan*

ARTICLE INFO

Article history:
Received 10 July 2009
Received in revised form 27 September 2009
Accepted 1 October 2009
Available online 9 October 2009

Keywords:
Amidase
Amidase signature family
Rhodococcus sp. N-771
Crystal structure
Substrate specificity

ABSTRACT

In this study, we have structurally characterized the amidase of a nitrile-degrading bacterium, *Rhodococcus* sp. N-771 (RhAmidase). RhAmidase belongs to amidase signature (AS) family, a group of amidase families, and is responsible for the degradation of amides produced from nitriles by nitrile hydratase. Recombinant RhAmidase exists as a dimer of about 107 kDa. RhAmidase can hydrolyze acetamide, propionamide, acrylamide and benzamide with *k*cat/*K*m values of 1.14 ± 0.23 $mM^{-1}s^{-1}$, 4.54 ± 0.09 $mM^{-1}s^{-1}$, 0.087 ± 0.02 $mM^{-1}s^{-1}$ and 153.5 ± 7.1 $mM^{-1}s^{-1}$, respectively. The crystal structures of RhAmidase and its inactive mutant complex with benzamide (S195A/benzamide) were determined at resolutions of 2.17 Å and 2.32 Å, respectively. RhAmidase has three domains: an N-terminal α-helical domain, a small domain and a large domain. The N-terminal α-helical domain is not found in other AS family enzymes. This domain is involved in the formation of the dimer structure and, together with the small domain, forms a narrow substrate-binding tunnel. The large domain showed high structural similarities to those of other AS family enzymes. The Ser-*cis* Ser-Lys catalytic triad is located in the large domain. But the substrate-binding pocket of RhAmidase is relatively narrow, due to the presence of the helix α13 in the small domain. The hydrophobic residues from the small domain are involved in recognizing the substrate. The small domain likely participates in substrate recognition and is related to the difference of substrate specificities among the AS family amidases.

1. Introduction

Nitrile compounds are widespread in the environment. In nature, they are present mainly as cyanoglycosides, which are produced by plants [1]. Plants also produce other nitrile compounds, such as cyanolipids, ricinine and phenylacetonitrile. Chemical industries make extensive use of nitrile compounds in the manufacture of a variety of polymers and other chemicals. Some microbes can grow on nitrile compounds. Microbial degradation of nitriles proceeds through two enzymatic pathways. Nitrilase catalyzes the direct cleavage of nitriles to the corresponding acids and ammonia, whereas nitrile hydratase catalyzes the hydration of nitriles to amides. Both nitrile-converting enzymes have attracted increasing attention as catalysts for processing organic chemicals [2–7]. Nitrile hydratase (NHase) is used as a catalyst in the production of acrylamide and is known as one of the most important industrial enzymes [8,9]. Generally, the NHase gene operon consists of the genes for the alpha and beta subunits of NHase, the NHase activator and amidase. The amides produced by NHase are degraded to their corresponding free carboxylic acids and ammonia by amidases [10].

Amidases (EC 3.5.1.4) have been classified [11–13] into two groups: the nitrilase superfamily and the amidase signature (AS) family. This division is based on the amino-acid sequence and structural similarities. Nitrilase superfamily enzymes exist as homo-tetrameric or homohexameric complexes in solution and have a conserved Glu, Cys and Lys catalytic triad in the catalytic center [14]. AS family enzymes form homodimeric or homooctameric complexes, and are characterized by a highly conserved stretch sequence of approximately 130 amino acids, the AS sequence, containing the Ser, Ser and Lys catalytic triad [10,11]. The biological functions and substrate specificities of AS family enzymes have been studied in detail [15–23]. However, only a few structures of AS family enzymes have been reported. The crystal structures of a Glutamyl-tRNA (Gln) amidotransferase subunit A [16], a fatty acid amide hydrolase [24], a peptide amidase (Pam) [25] and malonamidase E2 (MAE2) [26,27] have been determined. The structures of the AS sequence regions are

Abbreviations: AS, amidase signature; RhAmidase, *Rhodococcus* sp. N-771 amidase; S195A, mutant RhAmidase in which Ser195 is replaced by Ala; MAE2, *Bradyrhizobium japonicum* malonamidase; Pam, *Stenotrophomonas maltophilica* peptide amidase

* Corresponding author. Tel./fax: +81 42 388 7479.
E-mail address: yohda@cc.tuat.ac.jp (M. Yohda).

[1] These authors equally contributed to this work.

1570-9639/$ – see front matter © 2009 Elsevier B.V. All rights reserved.
doi:10.1016/j.bbapap.2009.10.001

conserved, and their unique feature, the Ser-*cis*Ser-Lys catalytic triad, is observed.

We have studied the structure and reaction mechanism of NHase from *Rhodococcus* sp. N771, which was used for the industrial production of acrylamide [8,28–30]. The NHase gene operon from *Rh*. sp. N771 contains the amidase gene. The amidase from *Rh*. sp. N-771 (RhAmidase) has all of the conserved amino acid residues in the Ser-*cis*Ser-Lys catalytic triad (S195-S171-K96) and the AS sequence. The sequence of the NHase operon from *Rh*. sp. N771 is identical to those of *Rh*. sp. N774 and *Rh*. sp. R312. Amidases of *Rh*. sp. N774 and *Rh*. sp. R312 have been expressed, purified and characterized [31,32]. They hydrolyzed propionamide efficiently, but their activities for acetamide, acrylamide and indoleacetamide were weak.

In this study, we have characterized RhAmidase and determined the crystal structure of RhAmidase at a resolution of 2.17 Å. We also determined the structure of the inactive mutant S195A complex with benzamide (S195A/benzamide) at a resolution of 2.32 Å. Based on the structures, we propose a molecular mechanism for substrate recognition.

2. Materials and methods

2.1. Construction of the expression plasmid

From the genomic DNA of *Rhodococcus* sp. N771, the gene for RhAmidase was amplified using Pfu polymerase with the primers, Fwd (5′-CATAGGCGACAATCCGACCT-3′) and Rev (5′-GAATTCCTAG-GCGGGGCT-3′). These primers contain the restriction sites for Nde I and EcoR I, respectively. The PCR products were subcloned into a pT7 Blue T vector (Novagen, Madison, WI). The plasmid for the expression of RhAmidase, pETAmi, was constructed by subcloning the Nde I/EcoR I fragment into the Nde I/EcoRI site of pET23b (Novagen). The inactive mutant S195A was constructed using the QuikChange Site-Directed Mutagenesis Kit (Stratagene, La Jolla, CA) and the plasmid pETAmi as the template. The oligonucleotides that were used to produce the S195A mutant were as follows, Fwd (5′-GATCAAGGAGCCATCCGGATCCCGGC-3′) and Rev (5′-GCCGGGATCCGGATGGCTCCGCCTTGATC-3′). The constructs were verified by DNA sequencing.

2.2. Preparation of RhAmidase

To produce RhAmidase, the expression vector (pETAmi) was introduced into *Escherichia coli* BL21 cells. The cells were grown at 37 °C in LB-broth for 18 hours. The harvested cells were suspended in buffer A (50 mM Tris-HCl, pH 8.0) and lysed by sonication. The cell debris was removed by centrifugation. The supernatant was applied to a DEAE-Toyopearl column (2.8×20 cm) (Tosoh, Tokyo, Japan) and the enzyme was eluted using a linear gradient of 0-500 mM NaCl in 300 mL of buffer A. The eluted enzyme was applied to a Butyl-Toyopearl column (2.8×10 cm) (Tosoh, Tokyo, Japan), and the enzyme was eluted using a 20-0% saturated ammonium sulfate gradient in 200 mL of buffer A. After dialysis against buffer A, the enzyme was loaded onto a Resource Q column (GE Healthcare, Buckinghamshire, UK) and eluted with 0-400 mM NaCl in 50 mL of buffer A. The inactive mutant, S195A, was purified in the same way as for wild type RhAmidase.

2.3. Size exclusion chromatography with multiangle light scattering (SEC-MALS)

The molecular mass of RhAmidase was determined in solution by SEC-MALS measurements using a JASCO HPLC system connected with a multiangle light-scattering detector (miniDAWN; Wyatt Technology, Santa Barbara, CA) and a differential refractive index detector (Shodex RI-101; Showa Denko, Tokyo, Japan). A TSKgel G3000SW$_{XL}$ column (Tosoh) was used with 50 mM Tris-HCl, pH 6.8 and 100 mM NaCl at a flow rate of 0.5 ml/min. Sample volumes of 100 µl were injected at a concentration of 1.0 mg/ml. The signal at the 90° angle was analyzed to obtain the weight-average molecular weight using the Astra software (Wyatt Technology).

2.4. The effects of pH and temperature on RhAmidase activity

The buffers used to determine the pH dependence of RhAmidase were: 200 mM sodium citrate (pHs 4.6 to 5.9), 200 mM potassium phosphate (pHs 5.8 to 7.7) and 200 mM Tris-HCl (pHs 6.8 to 8.8). Fifty microliters of purified RhAmidase, diluted to 0.15 mg/ml in the appropriate buffer, was mixed with 50 µl of 500 mM acrylamide, and the mixture was incubated for 5 min at 50 °C. Then, 100 µl of 1 M H_3PO_4 was added to stop the reaction. After centrifugation at 12,000 rpm for 10 min, 20 µl of the supernatant was injected into a C_{18} reverse-phase Spherisorb ODS-80TS (Tosoh) column on a HPLC system. Elution was done with 0.1% H_3PO_4 at a flow rate of 1.0 ml/min, and the formation of the corresponding carboxylic acids was detected by the absorbance at 210 nm. RhAmidase activities for the temperature dependence experiments were done at pH 5.9 over the temperature range from 20 to 70 °C. The kinetic parameters were determined using measurements made in triplicate for each set of conditions.

2.5. The amide hydrolysis activity assay

Amide hydrolysis activities for acetamide, propionamide, acrylamide and benzamide were determined by quantification of the carboxylic acids that were produced. We mixed 50 µl of purified RhAmidase with 50 µl of various concentrations of substrate in 200 mM sodium citrate pH 5.9 and incubated the mixture at 55 °C for 10 min. Then, 100 µl of 1 M H_3PO_4 was added to stop the reaction. The corresponding carboxylic acid products were separated and detected by HPLC with monitoring the absorbance at 210 nm. The kinetic parameters were obtained by applying the data to Michaelis-Menten equation directly using the KaleidaGraph program (Synergy Software).

Table 1
Diffraction data collection and refinement statistics.

	Wild-type RhAmidase	S195A/benzamide
Temperature (K)	100	100
Resolution (Å)	2.17	2.32
No. of measured refs.	239,364	184,861
No. of unique refs.	34,490	29,155
R_{merge}[a]	0.065 (0.296)[b]	0.052 (0.347)[b]
$I_o/\sigma(I_o)$	21.1 (5.4)[b]	16.9 (4.8)[b]
Completeness (%)	96.7 (99.0)[b]	99.5 (100)[b]
Space group	$P4_12_12$	$P4_12_12$
Cell dimensions		
a (Å)	92.672	92.272
b (Å)	92.672	92.272
c (Å)	162.305	161.799
Structure Refinement		
Resolution range (Å)	50.0–2.17	50.0–2.32
No. of refs.	34,490	29,155
R[c]	0.201	0.199
R_{free}[d]	0.232	0.233
Number of atoms		
Protein	3749	3749
Solvent	170	220
Ligand		9
r.m.s.d. bond lengths (Å)	0.005	0.006
r.m.s.d. bond angles (°)	1.3	1.3

[a] $R_{merge} = \Sigma_{hkl}\Sigma_i|I_i(hkl)-\langle I(hkl)\rangle|/\Sigma_{hkl}\Sigma I_i(hkl)$, where $I_i(hkl)$ is the *i*th intensity measurement of reflection hkl, including symmetry related reflections, and $\langle I(hkl)\rangle$ is its average.

[b] The values for the highest resolution shell are given in parentheses, (2.17-2.25 Å resolution for wild-type RhAmidase, 2.32-2.40 Å resolution for S195A/benzamide).

[c] $R = \Sigma_{hkl}(|F_o|-|F_c|)/\Sigma_{hkl}|F_o|$.

[d] R_{free} was calculated on 5% of the data omitted randomly [28].

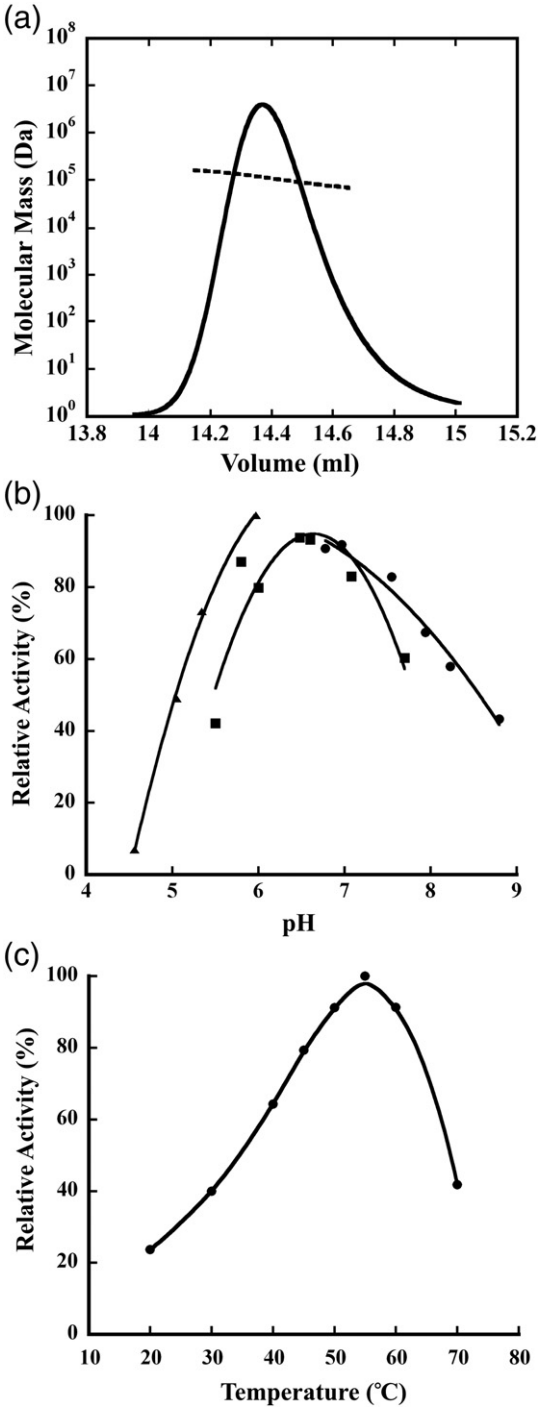

Fig. 1. Biochemical characterization of RhAmidase. (a) The SEC MALS measurement of RhAmidase. The average molecular mass per unit volume and the normalized refractive index (solid line) are shown. The theoretical mass of a dimer of RhAmidase is indicated by the dashed horizontal line. (b) The dependence of the hydrolytic activity of RhAmidase on pH. The assays were carried out as described in the text. The buffers that were used were: potassium citrate (pH 4.6-5.9; filled triangles), potassium phosphate (pH 5.8-7.7; filled squares) and Tris-HCl (pH 6.8-8.8; filled circles). (c) The temperature dependence of the hydrolytic activity of RhAmidase at pH 5.9. The maximum relative activity is indicated as 100%.

2.6. Crystallization and X-ray data collection

A crystal of RhAmidase was grown at 20 °C using the hanging drop vapor diffusion method by mixing 2 μL protein solution (14 mg/ml in 10 mM Tris-HCl, pH 8.0) and 2 μL reservoir solution (15% (w/v) polyethylene glycol 4000, 100 mM magnesium chloride, 100 mM calcium chloride, 100 mM MES (pH 6.0)). A crystal of S195A/benzamide was obtained using the co-crystallization method, a protein solution containing 10 mM benzamide and the same reservoir solution. The diffraction data were collected at 100 K using an ADSC CCD detector system on the BL5A beam line (wild type RhAmidase) at the Photon Factory and the MAR CCD detector on the BL38B beam line (S195A/benzamide) at SPring-8. The diffraction data were processed using the HKL2000 program [33].The statistics that resulted from the data processing and scaling are listed in Table 1.

2.7. Structure determination and refinement

The structure of wild type RhAmidase at 2.17 Å resolution was determined using the molecular replacement method and the Molrep program in the CCP4 program suite [34]. We used the partial structure of *Thermotoga maritime* Glutamyl-tRNA amidotransferase subunit A (residue 65-300 and 351-460, RCSB [35] PDB code 2gi3) as a probe model. The partial model that we used for molecular replacement shares 38% amino acid sequence identity with the corresponding region of RhAmidase. Further model building was performed using the X-fit program in the XtalView program system [36], and the structure was refined using the CNS program [37]. The models were corrected on the $(2F_o\text{-}F_c)$ electron density map, and we constructed the structure without solvent molecules using maximum resolution data. Solvent molecules were gradually introduced where peaks that had intensities that were greater than 4.0 σ in the $(F_o\text{-}F_c)$ electron density map were in the range of a hydrogen bond. To avoid over fitting the diffraction data, a free R factor was monitored with 5% of the test set excluded from the refinement [38]. The refinement statistics are shown in Table 1. After several cycles of refinement, we obtained a model with an *R*-factor of 0.201 (*R*free = 0.232).

The structure of S195A/benzamide was determined by molecular replacement using the structure of wild type RhAmidase and refined at a resolution of 2.32 Å. Before adding the water molecules, the benzamide molecule was placed in the active site. Water molecules were added, and the structure was refined in the same manner as for wild type RhAmidase. Finally, the structure of the S195A/benzamide complex was refined to an *R*-factor of 0.199 (*R*free = 0.232). The atomic coordinates and structure factors for RhAmidase and the S195A/benzamide complex have been deposited in the PDB under accession codes 3A1 K and 3A1I, respectively.

3. Results and discussion

3.1. Properties of recombinant RhAmidase

Because members of the AS family are known to exist as homodimeric or homooctameric oligomers, we investigated the oligomeric state of RhAmidase in solution using size-exclusion chromatography combined with multiangle light scattering (SEC-MALS) (Fig. 1(a)). SEC-MALS measurement of RhAmidase provides a molecular mass (MM) of 107.0 kDa, which is in good agreement with the MM of the dimer as calculated from the deduced MM of the monomer, 54.7 kDa.

The purified RhAmidase could hydrolyze acrylamide between pH 5.0 and 8.8, and the optimum was at pH 5.9 (sodium citrate buffer,

Table 2
Kinetic parameters of RhAmidase.

Compound	Km (mM)	kcat (s^{-1})	kcat/Km (s^{-1} mM^{-1})
Acetamide	19.0 ± 6.3	20.2 ± 2.9	1.14 ± 0.23
Propionamide	34.2 ± 1.2	155.3 ± 8.2	4.54 ± 0.09
Acrylamide	24.1 ± 11.9	2.10 ± 1.04	0.087 ± 0.02
Benzamide	1.03 ± 0,05	157.7 ± 3.4	153.5 ± 7.1

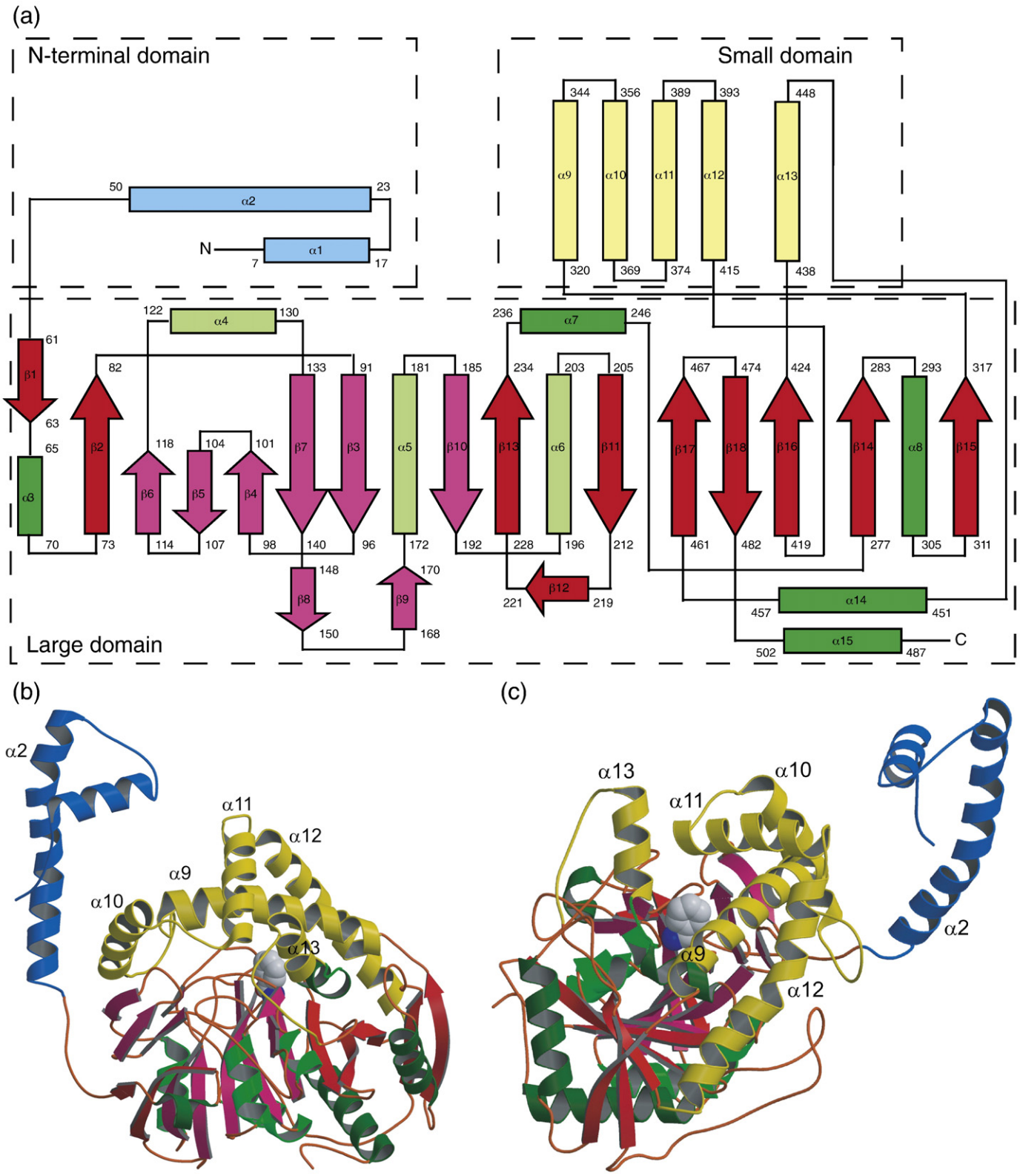

Fig. 2. Crystal structure of RhAmidase. (a) A topological diagram showing the arrangement of the secondary structure units of RhAmidase. The β-sheet and α-helices in the AS family signature sequence and the other β-sheet and α-helices in the α/β domain are shown in light green, magenta, green and red, respectively. The N-terminal and small domain are shown in blue and yellow, respectively. The overall monomer structure of S195A/benzamide showing (b) the side view and (c) the top view and (d) the dimer structure, as illustrated using MOLSCRIPT [40] and Raster3D [41]. RhAmidase, with a space group of $P4_12_12$, has one molecule in the asymmetric unit. The biologically active dimer is derived by applying crystallographic symmetry rules. A single monomer is shown and colored as described in panel (a). The symmetrical molecule is shown in grey. Note the extended α-helical N-terminal domain interacting with the other monomer. The bound benzamide is shown by the CPK model.

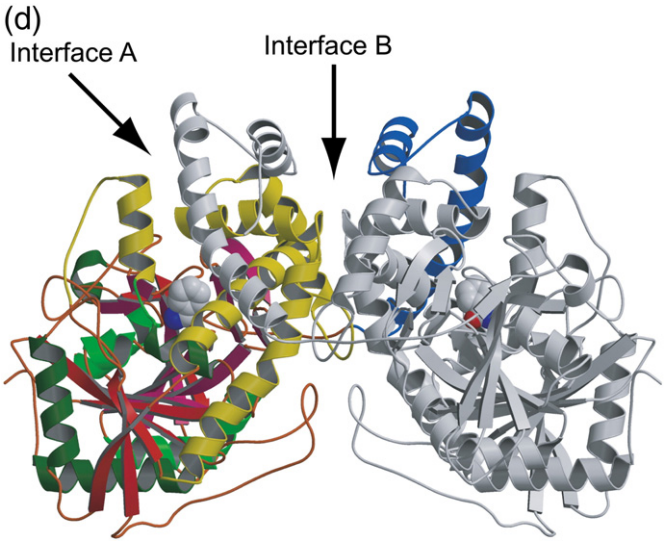

Fig. 2 (*continued*).

Fig. 1(b)). The activity was determined between 40 and 60 °C, and the maximum was at 55 °C. Above 60 °C, the activity decreased sharply (Fig. 1(c)).

The kinetic parameters of RhAmidase for the amide compounds (acetamide, propionamide, acrylamide and benzamide) were calculated (Table 2). The *K*m values of three small amide compounds (acetamide, propionamide and acrylamide) are relatively high compared with that of benzamide. The k_{cat} values are significantly different among these substrates. The *k*cat/*K*m values were calculated to be 1.14 ± 0.23 $mM^{-1}s^{-1}$, 4.54 ± 0.09 $mM^{-1}s^{-1}$, 0.087 ± 0.02 $mM^{-1}s^{-1}$, and 153.5 ± 7.1 $mM^{-1}s^{-1}$, respectively. The most preferable substrate is benzamide, and acrylamide was poorly catalyzed. These results are similar to those of the amidase from *Rh.* sp. R312 [31].

3.2. Structural determination of RhAmidase

The crystal structure of wild type RhAmidase was determined at 2.17 Å resolution. We then attempted to determine the structures of the RhAmidase complexed with acrylamide, propionamide or benzamide using an inactive variant in which Ser195 was replaced by Ala (S195A). The S195A mutation impairs the hydrolysis activity for each substrate completely. Although we were able to obtain crystals of the complexes with acrylamide and propionamide and diffraction data, we were unable to interpret the electron density maps of the acrylamide and propionamide due to the ambiguous electron density. The problem appears to result from the small side-chains of these substrates. On the other hand, the electron density map of benzamide was visible in the structure of S195A complex with benzamide (S195A/benzamide), and we could determine the positions of the side chains and the amide accurately. Finally, we could determine the crystal structure of S195A in a complex with benzamide at 2.32 Å resolution.

The crystal structures of RhAmidase and S195A/benzamide, with a space group of $P4_12_12$, both have one molecule with 508 residues (2-509) of the 521 residues in the asymmetrical unit. The first N-terminal residue, Met1, was probably deleted by processing in *E. coli*, and the last C-terminal 12 residues appear disordered. The final (2*F*o-*F*c) electron density maps of both crystal structures (contoured at1 σ) showed that all atoms of the proteins, benzamide and solvent molecules were well fitted. We analyzed the stereochemical quality of the models using the program PROCHECK [39]. The structures were refined to an *R*work/*R*free [38] of 0.201/0.233 (RhAmidase) and 0.199/0.232 (S195A/benzamide).

3.3. The overall structure of wild type RhAmidase and S195A/benzamide

A topological diagram showing the secondary structure of RhAmidase is presented in Fig. 2(a). The r.m.s. deviation for the Cα atoms between wild type RhAmidase and S195A/benzamide is 0.43 Å. The binding of benzamide did not cause significant displacement of the amino acid residues. Hereafter, we describe the structure of RhAmidase using that of S195A/benzamide. The overall structure of S195A/benzamide is shown in Fig. 2(b) and (c). The refined model of RhAmidase has 15 α-helices and 18 β-strands. In the structure, 41% of the residues occur in α-helices and 21% of the residues occur in β-strands. The structure of RhAmidase can be divided into three domains (Fig. 2(b)): the α-helical N-terminal domain, and the large and small domains. The large and small domains form the core structure. The large domain has a α/β structure, consisting of a hydrophobic core of an 18 β-stranded β-sheet structure, with 8 α-helices located on both sides of the β-sheet. The large domain contains an AS sequence (residues 95-204), which forms the bottom of the active site and is topologically homologous to known amidase structures. The small domain has 5 helices (α9, α10, α11, α12 and α13) located on the top of the large domain and 4 helices (α9-α12) that are connected by short segments, forming a helix-turn-helix motif-like structure. The α-helical N-terminal domain consists of residues 2-53 and forms two α-helices. This N-terminus α-helix is isolated from the core structure, but it interacts with the small domain of the other monomer in the dimer, as discussed below.

3.4. The dimer structure of RhAmidase

The crystal structures of wild type RhAmidase and S195A/benzamide in the asymmetric unit both form a dimer structure related by the 2-fold crystallographic axis. The dimerization interface is composed of two parts that interact through α−helices (interfaces A and B, Fig. 2(d)). At the interface A, the N-terminal α-helical domain (residues 2-53) participates in the main dimer interaction of RhAmidase. Helix α2′ (residue 23-50) of the N-terminal domain of its dimeric partner is covered by the groove that is formed by α9, α11 and α13 of the small domain. This helix hinders the exposure of the solvent accessible surface. In addition, at the interface B, part of helix α10 faces towards helix α2′ and α12′ of its dimeric partner. In the dimer structure, the exposed surface area is 31,835 $Å^2$ and the buried surface area is 9,603 $Å^2$. These results show that the N-terminal domain and all helices of the small domain participate in forming the dimer structure and that these interactions contribute to the formation of a closely packed dimer structure. SEC-MALS measurement of RhAmidase suggested that the quaternary structure of this enzyme is a dimer structure, as mentioned above. This dimer structure in the crystal is thought to be the same as the biologically active dimer structure in solution. Every available amidase structure has an α/β large domain that includes AS-specific sequence. However, the position of the extended N-terminal domain in other amidase structures is different from that of RhAmidase, in which it forms a part of the core domain. The interaction of the N-terminal domain in the core domain is thought to be the main driving force for dimerization, which results in the novel amidase architecture.

3.5. The catalytic residues of RhAmidase

The active site is located in the middle of the core structure. Structural and biochemical studies of AS family amidases have shown that three residues are essential for substrate hydrolysis. In RhAmidase, these residues are Ser171, Ser195 and Lys96. Fig. 3(a) and (b) show the omit map for the binding of benzamide and the interactions between the enzyme and the bound benzamide. Ser171 is in the middle of the highly conserved Gly and Ser-rich loop region (G169-G170-S171-S172-G173-G174). Ser171 is in an unusual *cis*

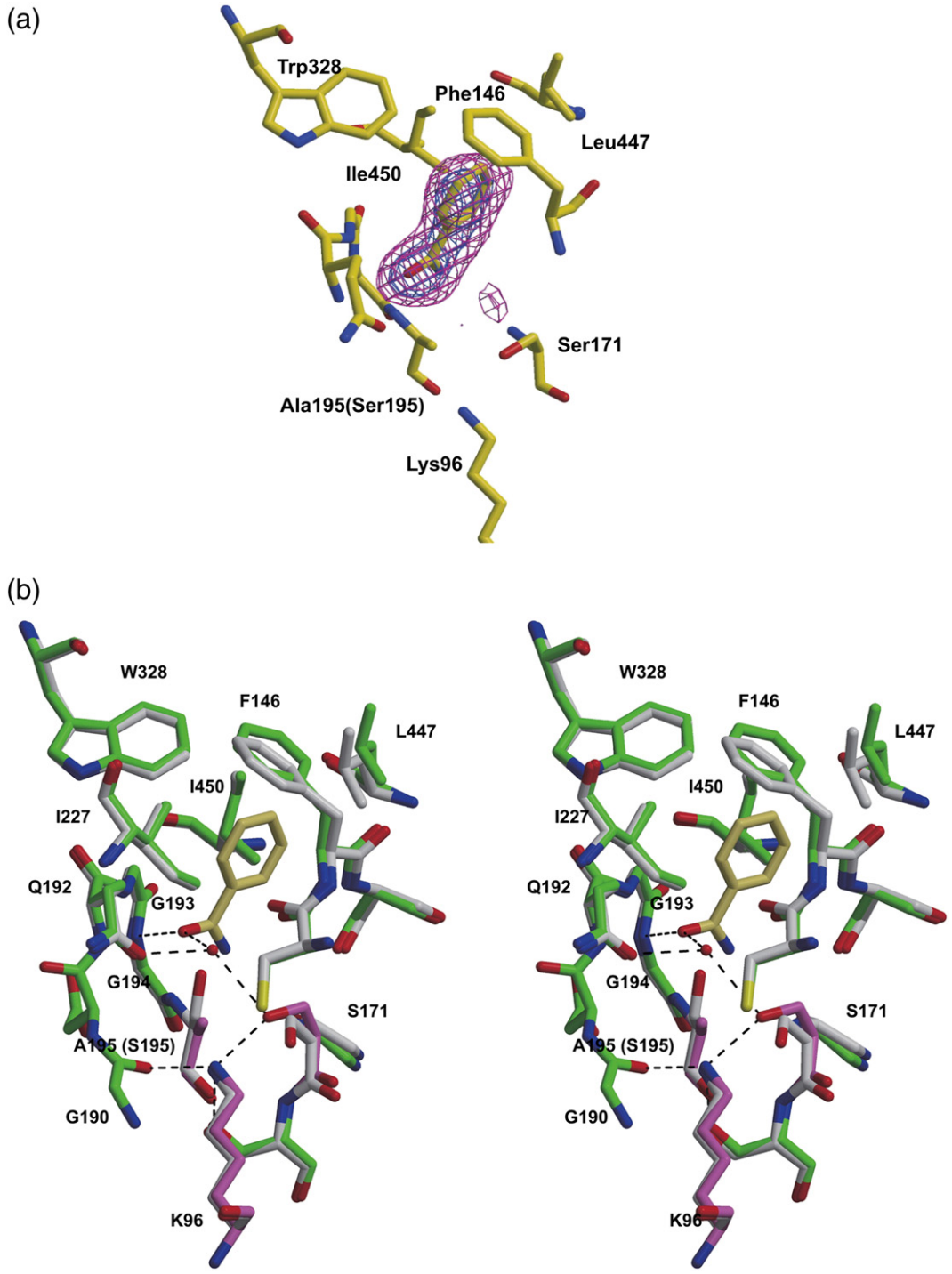

Fig. 3. The structure of the active site of RhAmidase. (a) The simulated annealing omit map of the bound benzamide in the S195A/benzamide complex. The contour level of the maps is 4 σ (magenta) and 7 σ (blue). (b) A stereoview of the superposition of the Cα atoms at the active site of wild type RhAmidase (grey) and the S195A/benzamide (green) complex structure, as illustrated using the programs MOLSCRIPT [40] and Raster3D [41]. Selected hydrogen bonds are depicted using dotted lines and the carbon atoms of the bound benzamide and the three catalytic residues are shown in yellow and magenta, respectively.

conformation (Fig. 3(b)), which is conserved in other AS family enzymes [16,19,26,27]. Lys96 is in direct contact with the Oγ atom of *cis*Ser171 (2.9 Å). In addition, Lys96 makes hydrogen bonds with the Oγ atom of Ser172 (3.0 Å) and the O atom of Gly190 (3.2 Å), which are conserved in AS family enzymes. Thus, Lys96 and this hydrogen-bonding network likely play a role in maintaining the orientation of *cis*Ser171. Superimposing the structures of the wild type and the S195A/benzamide complex shows that the substrate amide carbon is 1.9 Å from the Ser195 Oγ atom (Fig. 3(b)). Therefore, Ser195 should form a covalent bond with the substrate. This observation suggests that Ser195 acts as the nucleophile and forms a covalent substrate-enzyme intermediate in the course of the catalysis of RhAmidase. This covalent modification of Ser is also observed in the structure of MAE2 [26,27] and GatAB [16]. Ser155 of MAE2 and Ser178 of GatAB form tight covalent bonds with a pyrophosphoryl group and glutamine, respectively.

3.6. Benzamide binding to the active site

The active site is formed by residues in the loops between β3 and β4 (residues 96-98), β7 and β8 (145-148), β9 and α5 (170-172), β10 and α6 (192-195) and β12 and β13 (222-224) from the large domain, and a part of helix α13 (446-450) and α9 (328-338) from the small domain. There are no hydrophilic residues in the active site, except for the catalytic residues. Being surrounded by the hydrophobic residues Phe146, Ile227, Trp328, Leu447 and Ile450, the active site is narrow and hydrophobic.

Phe146, Ile227, Trp328, Leu447 and Ile450 make hydrophobic interactions with the benzene ring of benzamide. In this binding mode, the conformations of the side chains of Phe146 and Leu447 are slightly different to those found in wild type RhAmidase; Phe146 is close to the benzamide and Leu447 is apart from it, forming favorable hydrophobic interactions. These residues may change their side chain conformations to recognize the substrate, depending on the size or shape of the substrate. The oxyanion hole, i.e., the four backbone nitrogen atoms of Gln192 (2.9 Å), Gly193 (2.6 Å), Gly194 (3.3 Å) and Ala195 (3.2 Å), interact directly with the amide oxygen of benzamide. This suggests that these interactions stabilize the enzyme-substrate intermediate during RhAmidase catalysis. Other residues that aid in forming the active site cleft do not form contacts with benzamide. These observations show that residues 192-195 are essential for benzamide recognition.

3.7. The contribution of the N-terminal domain to the formation of the substrate pathway in RhAmidase

Sequence analyses have shown that the N-terminal domain of amidases is found in amidases from some *Rhodococcus* sp. and in other bacterial amidases. However, a correlation between the N-terminal domain and the functional properties of these amidases has not been examined. The sequence of the N-terminal domain does not share high homology with any other proteins. We investigate here the contribution of the N-terminal domain to substrate specificity using structural analysis.

The substrate pathway formed by α9, α11 and α13, is observed clearly on the surface of the structure of the RhAmidase monomer (Fig. 4(a)). However, in the dimeric structures of wild type RhAmidase and the S195A/benzamide complex, the N-terminal domain of the dimeric partner is located far above the active site, covering the substrate pathway (Figs. 2(d) and 4(b)). As a result of dimer formation, the exposed surface area of the monomer interface (2184 Å^2) is reduced to 1044 Å^2, and the width of the entrance of the substrate pathway is reduced from 17 Å to about 8 Å. These observations suggest that RhAmidase might show a preference for small amide compounds as substrates. However, experimental results show that RhAmidase has a low activity for short chain amides. As shown in Fig. 3(a), the hydrophobic residues (Phe146, Ile227, Trp328, Leu447 and Ile450) recognize the benzene ring of benzamide using van der Waals (VDW) interactions. Using the S195A/benzamide structure, we modeled the structures of the complexes with acetamide, acrylamide and propionamide. In the modeled structures, the methyl, ethylene and ethyl group of these amide compounds made no VDW interactions with the hydrophobic residues, and this is most likely the reason for the low activity of these three amide compounds. Thus, RhAmidase may have very selective substrate specificities that originate from its narrow hydrophobic pocket, substrate pathway and recognition mechanism.

3.8. Comparison with other AS family amidases

RhAmidase exhibits low amino acid sequence homology with other AS family proteins in the PDB (*Bradyrhizobium japonicum* malonamidase (MAE2, PDB code; 1ock, 20% sequence identity) [26],

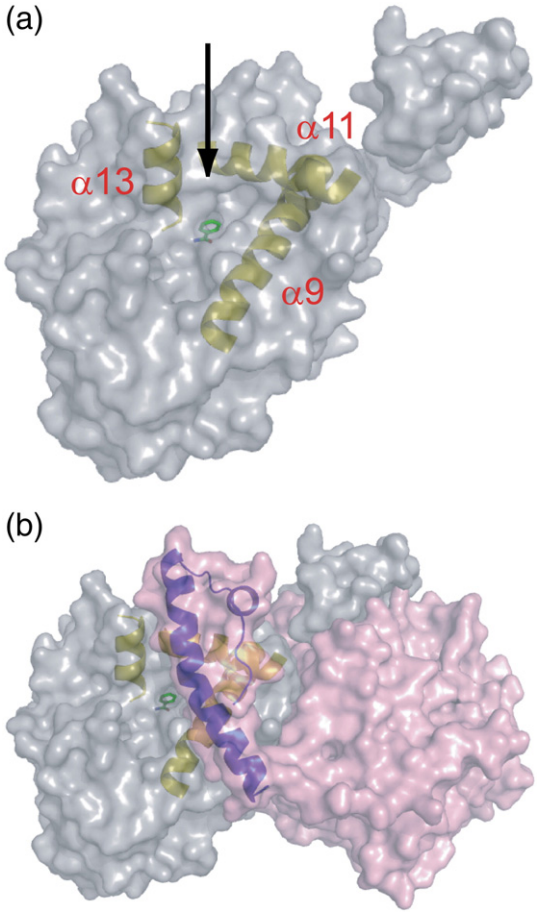

Fig. 4. The surface of the active site of S195A/benzamide. An overview of the structure of the surface of the active site of (a) the monomer and (b) the dimer of S195A/benzamide, as illustrated using the program Pymol [42]. Helices α9 (residues; 320-344), α11 (374-389) and α13 (438-448) are shown using ribbon models. Helix α2′ from the dimeric partner is shown in purple. The bound benzamide, located at the bottom of active site, is shown using a ball-and-stick model.

Stenotrophomonas maltophilica peptide amidase (Pam, PDB code; 1m22, 23% sequence identity) [25], *Staphylococcus aureus* glutamine amidotransferase subunit A (PDB code; 2g5i, 25% sequence identity) [16] and *Thermotoga maritima* Glutamyl-tRNA amidotransferase subunit A (PDB code; 2gi3, 28% sequence identity). In spite of the low amino acid sequence identity, the overall folding of these enzymes was similar to RhAmidase except for the N-terminal domain. As the large domain includes an AS sequence with high sequence homology and structural similarities, the substrate specificities would depend on the substantial variation in the number and composition of amino acids in the small domain. In fact, in RhAmidase, three hydrophobic residues (Trp328, Leu447 and Ile450) from the small domain are involved in substrate recognition that are not conserved in other AS family enzymes. Comparison of the structure of RhAmidase with other AS family amidases (MAE2 and Pam) shows that the substrate-binding pocket of RhAmidase is much narrower (Fig. 5(a)). This is partly due to the presence of helix α13 (residues 438-450) in RhAmidase. In both MAE2 (354-359) and Pam (463-468), this is a loop region. This wide, open substrate-binding pocket of Pam accounts for its substrate specificity for peptide amides, which are large amide compounds. In MAE2, despite the small and hydrophilic substrate (malonamate), the substrate-binding pocket remains wide and open. However, the large hydrophilic residues, Arg113 and Arg158 (MAE2 numbering), which are not conserved in the AS sequence, protrude from the large domain, rather than helix α13 of RhAmidase. Other large residues (Tyr183, His273 and Gln277) from

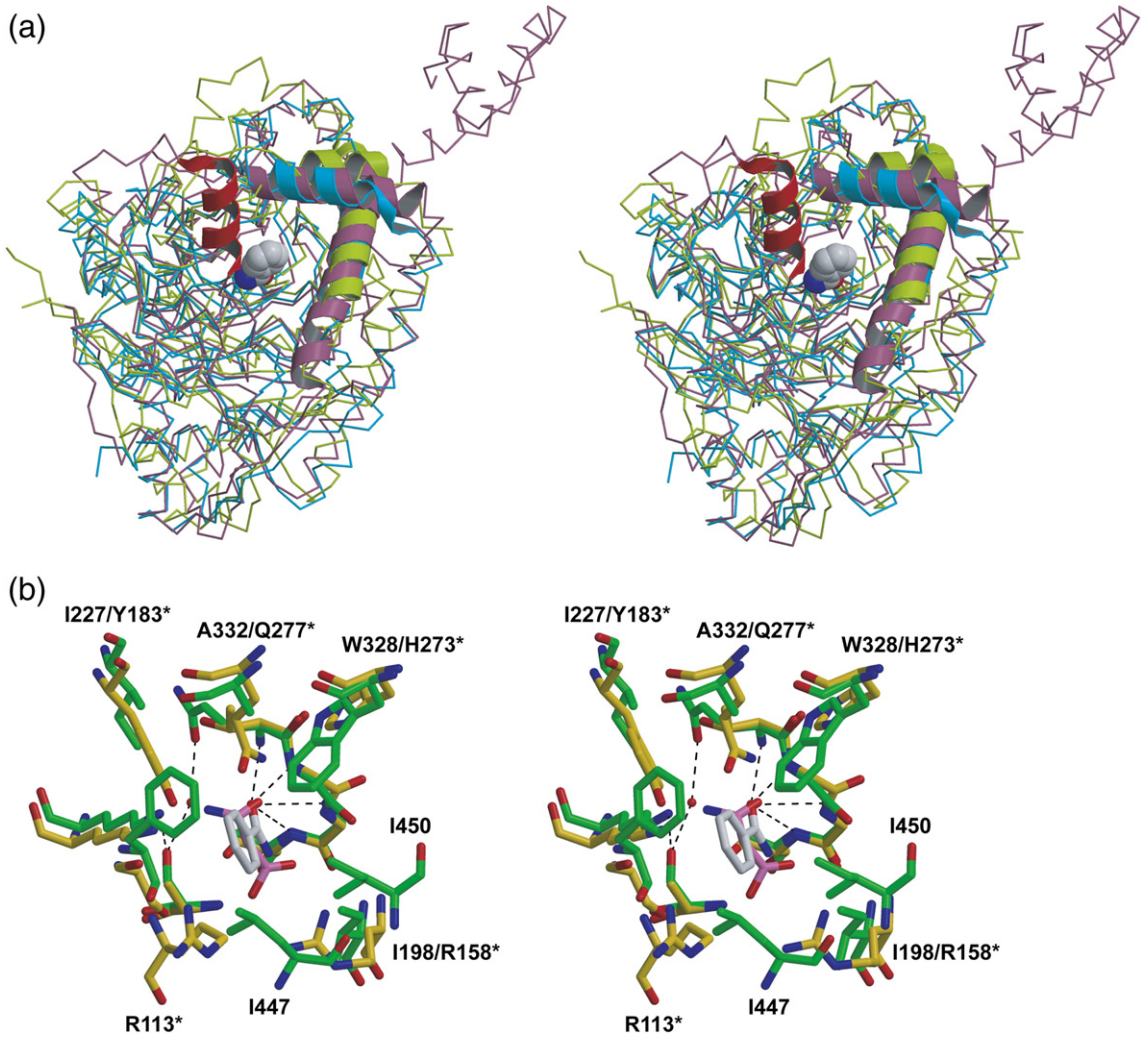

Fig. 5. A structural comparison between the members of the AS family amidases. (a) A stereoview of the superposition of the Cα models of RhAmidase (pink), Pam (green) and MAE2 (cyan). Helices α9 (residues; 320-344), α11 (374-389) and α13 (438-448) are shown using ribbon models, and the helices that occupy the equivalent positions to α9 (residues 356-379 in Pam and 272-284 in MAE2) and α11 (402-415 in Pam and 299-311 in MAE2) of Pam and MAE2 are also shown using ribbon models. Helix α13 of RhAmidase is shown in red. The bound benzamide is depicted using a mesh-model. (b) A stereoview of the superposition of the Cα atoms of the oxyanion hole (residues 192-195) at the active site of the S195A/benzamide complex (green) and the MAE2/malonamate complex (yellow) structure. The bound benzamide in the S195A/benzamide complex and the malonamate in MAE2/malonamate complex structure are shown in grey and magenta, respectively. The residue number of MAE2 is labeled with "*".

the small domain form a hydrophilic, narrow active site that recognizes malonamate, as shown in Fig. 5(b). Thus, the small domain clearly participates in substrate recognition and is responsible for the different substrate specificities in the AS family of amidases.

Here, we have reported the preliminary characterization and crystal structure of RhAmidase, and we propose the substrate recognition mechanism. However, we could not obtain detailed information about the structure-function relationship, e.g., why the hydrolytic activity of RhAmidase should be so different between propionamide and acrylamide. Further biochemical studies are necessary to provide more detailed information about the catalytic mechanism and the substrate specificities of the AS family of enzymes.

Acknowledgements

We are grateful to the beamline assistants at the Photon Factory (PF) for data collection at beamline BL-5A. We also thank Drs. Yuki Nakamura, Go Ueno, Takaaki Hikima and Masaki Yamamoto for the automated data collection at Spring-8 using the mail-in system. The work reported here is part of the support program for improving graduate school education of the "Human Resource Development Program for Scientific Powerhouse", which is financially supported by the Ministry of Education, Culture, Sports, Science and Technology in Japan through Tokyo University of Agriculture & Technology. This work was also supported partly by a Grant-in-Aid for Scientific Research (B) (19350080) (to M. O.) from the Japanese Society for the Promotion of Science (JSPS), and a grant of the National Project on Protein Structural and Functional Analyses from the Ministry of Education, Science, Sports and Culture of Japan (to M. Y.).

References

[1] S.S. Thayer, E.E. Conn, Subcellular Localization of Dhurrin beta-Glucosidase and Hydroxynitrile Lyase in the Mesophyll Cells of Sorghum Leaf Blades, Plant. Physiol. 67 (1981) 617–622.
[2] M. Gao, D.X. Wang, Q.Y. Zheng, Z.T. Huang, M.X. Wang, Remarkable electronic and steric effects in the nitrile biotransformations for the preparation of enantiopure functionalized carboxylic acids and amides: implication for an unsaturated carbon-carbon bond binding domain of the amidase, J. Org. Chem. 72 (2007) 6060–6066.
[3] D.Y. Ma, D.X. Wang, J. Pan, Z.T. Huang, M.X. Wang, Nitrile biotransformations for the synthesis of highly enantioenriched beta-hydroxy and beta-amino acid and amide derivatives: a general and simple but powerful and efficient benzyl protection strategy to increase enantioselectivity of the amidase, J. Org. Chem. 73 (2008) 4087–4091.
[4] L. Song, M. Wang, J. Shi, Z. Xue, M.X. Wang, S. Qian, High resolution X-ray molecular structure of the nitrile hydratase from Rhodococcus erythropolis AJ270 reveals posttranslational oxidation of two cysteines into sulfinic acids and a novel

biocatalytic nitrile hydration mechanism, Biochem. Biophys. Res. Commun. 362 (2007) 319–324.
[5] J.Y. Wang, D.X. Wang, J. Pan, Z.T. Huang, M.X. Wang, Nitrile and amide biotransformations for the synthesis of enantiomerically pure 3-arylaziridine-2-carboxamide derivatives and their stereospecific ring-opening reactions, J. Org. Chem. 72 (2007) 9391–9394.
[6] M.X. Wang, Enantioselective Biotransformations of Nitriles in Organic Synthesis Topics in Catalysis 35 (2005) 117-130.
[7] M.X. Wang, Progress of Enantioselective Nitrile Biotransformations in Organic Synthesis Chimia 63 (2009) 331-333.
[8] I. Endo, M. Nojiri, M. Tsujimura, M. Nakasako, S. Nagashima, M. Yohda, M. Odaka, Fe-type nitrile hydratase, J. Inorg. Biochem. 83 (2001) 247–253.
[9] H. Yamada, M. Kobayashi, Nitrile hydratase and its application to industrial production of acrylamide, Biosci. Biotechnol. Biochem. 60 (1996) 1391–1400.
[10] J.F. Mayaux, E. Cerbelaud, F. Soubrier, P. Yeh, F. Blanche, D. Petre, Purification, cloning, and primary structure of a new enantiomer-selective amidase from a Rhodococcus strain: structural evidence for a conserved genetic coupling with nitrile hydratase, J. Bacteriol. 173 (1991) 6694–6704.
[11] H. Chebrou, F. Bigey, A. Arnaud, P. Galzy, Study of the amidase signature group, Biochim. Biophys. Acta 1298 (1996) 285–293.
[12] D. Fournand, A. Arnaud, Aliphatic and enantioselective amidases: from hydrolysis to acyl transfer activity, J. Appl. Microbiol. 91 (2001) 381–393.
[13] H.C. Pace, C. Brenner, The nitrilase superfamily: classification, structure and function, Genome. Biol. 2 (2002) REVIEWS0001.1-0001.9.
[14] S.I. Pertsovich, D.T. Guranda, D.A. Podchernyaev, A.S. Yanenko, V.K. Svedas, Aliphatic amidase from Rhodococcus rhodochrous M8 is related to the nitrilase/cyanide hydratase family, Biochemistry. (Mosc) 70 (2005) 1280–1287.
[15] A.W. Curnow, K. Hong, R. Yuan, S. Kim, O. Martins, W. Winkler, T.M. Henkin, D. Soll, Glu-tRNAGln amidotransferase: a novel heterotrimeric enzyme required for correct decoding of glutamine codons during translation, Proc. Natl. Acad. Sci. U. S. A. 94 (1997) 11819–11826.
[16] A. Nakamura, M. Yao, S. Chimnaronk, N. Sakai, I. Tanaka, Ammonia channel couples glutaminase with transamidase reactions in GatCAB, Science 312 (2006) 1954–1958.
[17] A. Schon, C.G. Kannangara, S. Gough, D. Soll, Protein biosynthesis in organelles requires misaminoacylation of tRNA, Nature 331 (1988) 187–190.
[18] B.F. Cravatt, D.K. Giang, S.P. Mayfield, D.L. Boger, R.A. Lerner, N.B. Gilula, Molecular characterization of an enzyme that degrades neuromodulatory fatty-acid amides, Nature 384 (1996) 83–87.
[19] D.G. Deutsch, N. Ueda, S. Yamamoto, The fatty acid amide hydrolase (FAAH), Prostaglandins, Leukot. Essent. Fat. Acids 66 (2002) 201–210.
[20] B. Koutek, G.D. Prestwich, A.C. Howlett, S.A. Chin, D. Salehani, N. Akhavan, D.G. Deutsch, Inhibitors of arachidonoyl ethanolamide hydrolysis, J. Biol. Chem. 269 (1994) 22937–22940.
[21] R.L. Omeir, G. Arreaza, D.G. Deutsch, Identification of two serine residues involved in catalysis by fatty acid amide hydrolase, Biochem. Biophys. Res. Commun. 264 (1999) 316–320.
[22] T.D. Gaffney, O. da Costa e Silva, T. Yamada, T. Kosuge, Indoleacetic acid operon of Pseudomonas syringae subsp. savastanoi: transcription analysis and promoter identification, J. Bacteriol. 172 (1990) 5593–5601.
[23] K. Gomi, K. Kitamoto, C. Kumagai, Cloning and molecular characterization of the acetamidase-encoding gene (amdS) from Aspergillus oryzae, Gene 108 (1991) 91–98.
[24] M.H. Bracey, M.A. Hanson, K.R. Masuda, R.C. Stevens, B.F. Cravatt, Structural adaptations in a membrane enzyme that terminates endocannabinoid signaling, Science 298 (2002) 1793–1796.
[25] J. Labahn, S. Neumann, G. Buldt, M.R. Kula, J. Granzin, An alternative mechanism for amidase signature enzymes, J. Mol. Biol. 322 (2002) 1053–1064.
[26] S. Shin, T.H. Lee, N.C. Ha, H.M. Koo, S.Y. Kim, H.S. Lee, Y.S. Kim, B.H. Oh, Structure of malonamidase E2 reveals a novel Ser-cisSer-Lys catalytic triad in a new serine hydrolase fold that is prevalent in nature, EMBO J. 21 (2002) 2509–2516.
[27] S. Shin, Y.S. Yun, H.M. Koo, Y.S. Kim, K.Y. Choi, B.H. Oh, Characterization of a novel Ser-cisSer-Lys catalytic triad in comparison with the classical Ser-His-Asp triad, J. Biol. Chem. 278 (2003) 24937–24943.
[28] K. Hashimoto, H. Suzuki, K. Taniguchi, T. Noguchi, M. Yohda, M. Odaka, Catalytic mechanism of nitrile hydratase proposed by time-resolved X-ray crystallography using a novel substrate, tert-butylisonitrile, J. Biol. Chem. 283 (2008) 36617–36623.
[29] M. Odaka, T. Noguchi, S. Nagashima, M. Yohda, S. Yabuki, M. Hishino, Y. Inoue, I. Endo, Location of the non-heme iron center on the alpha subunit of photoreactive nitrile hydratase from Rhodococcus sp. N-771, Biochem. Biophys. Res. Commun. 221 (1996) 146–150.
[30] K. Taniguchi, K. Murata, Y. Murakami, S. Takahashi, T. Nakamura, K. Hashimoto, H. Koshino, N. Dohmae, M. Yohda, T. Hirose, M. Maeda, M. Odaka, Novel catalytic activity of nitrile hydratase from Rhodococcus sp. N771, J. Biosci. Bioeng. 106 (2008) 174–179.
[31] D. Fournand, F. Bigey, A. Arnaud, Acyl transfer activity of an amidase from Rhodococcus sp. strain R312: formation of a wide range of hydroxamic acids, Appl. Environ. Microbiol. 64 (1998) 2844–2852.
[32] Y. Hashimoto, M. Nishiyama, O. Ikehata, S. Horinouchi, T. Beppu, Cloning and characterization of an amidase gene from Rhodococcus species N-774 and its expression in Escherichia coli, Biochim. Biophys. Acta 1088 (1991) 225–233.
[33] Z.A.M. Otwinowski, Processing of X-ray Diffraction Data Collected in Oscillation Mode, Methods Enzymol Macromol. Crystallogr., part A 276 (1997) 307–326.
[34] N. Collaborative Computational Project, The CCP4 Suite: Programs for Protein Crystallography, Acta Cryst. D 50 (1994) 760–763.
[35] H.M. Berman, J. Westbrook, Z. Feng, G. Gilliland, T.N. Bhat, H. Weissig, I.N. Shindyalov, P.E. Bourne, The Protein Data Bank, Nucleic Acids Res. 28 (2000) 235–242.
[36] D.E. McRee, XtalView/Xfit–A versatile program for manipulating atomic coordinates and electron density, J. Struct. Biol. 125 (1999) 156–165.
[37] A.T. Brunger, P.D. Adams, G.M. Clore, W.L. DeLano, P. Gros, R.W. Grosse-Kunstleve, J.S. Jiang, J. Kuszewski, M. Nilges, N.S. Pannu, R.J. Read, L.M. Rice, T. Simonson, G.L. Warren, Crystallography & NMR system: A new software suite for macromolecular structure determination, Acta Crystallogr. 54 (1998) 905–921.
[38] A.T. Brunger, Free R value: a novel statistical quantity for assessing the accuracy of crystal structures, Nature 355 (1992) 472–475.
[39] M.M.W. Laskowski, R AMoss D S , ThorntonJM , A program to check the stereochemical quality of protein structures, J. Appl. Cryst. 26 (1993) 283–291.
[40] P.J. Kraulis, MOLSCRIPT: A Program to Produce Both Detailed and Schematic Plots of Protein Structures, J. Appl. Crystallogr. 24 (1991) 946–950.
[41] E.A. Merritt, D.J. Bacon, Raster3D: photorealistic molecular graphics, Methods Enzymol. 277 (1997) 505–524.
[42] W.L. DeLano, The PyMOL Molecular Graphics System, DeLano Scientific, Palo Alto, CA, USA, 2002.